ANL/RA/CP- 94968

Paper to be presented at the ASME/JSME/SFEN 6th International Conference on Nuclear Engineering, May 10-15, 1998, San Diego CA

MSET MODELING OF CRYSTAL RIVER-3 VENTURI FLOW METERS

J. P. Herzog
S. W. Wegerich
K. C. Gross
Reactor Analysis Division
Argonne National Laboratory
9700 S. Cass Avenue
Argonne, IL 60439

and

F. K. Bockhorst
Nuclear Plant Systems Engineering
Florida Power Corp.
P.O. Box 219
Crystal River, FL

Work supported by the U. S. Department of Energy, Nuclear Energy Programs under Contract W-31-109-Eng-38

DISCLAIMER

DISCLAIMER

Portions of this document may be illegible in electronic image products. Images are produced from the best available original document.

6th International Conference on Nuclear Engineering
ICONE-6
May 10-15, 1998

MSET MODELING OF CRYSTAL RIVER-3 VENTURI FLOW METERS

J. P. Herzog, S. W. Wegerich, K. C. Gross
Argonne National Laboratory
Reactor Analysis Division
9700 South Cass Avenue
Argonne, IL, USA, 60439-4842

F. K. Bockhorst
Florida Power Corporation
15760 W. Power Line Street
Crystal River, FL, USA, 34428-6708

Introduction

One of the primary objectives of nuclear power plants is the efficient operation of plant systems, thereby reducing the cost of electricity. Accurate determination of the thermal power of the plant is needed to minimize the offset required between safety trips and operating point and to thereby help minimize the cost per unit of energy produced. Currently, classical thermodynamic methods utilizing mass and energy balances on the plant steam generators are used for the thermal power calculation. The feedwater flow rate to the steam generators is one of the primary quantities used for the calculation of a reactor's thermal power. However, the accuracy of the venturi flow meters that measure the feedwater flow rate can deteriorate over time due to a buildup of corrosion products on the inner surface of the flow meter. This flow meter fouling may result in flow rate measurements that are higher than their actual values, yielding artificially high thermal powers (Kavaklioglu and Upadhyaya, 1994). U. S. NRC licensing rules require that the calculated thermal power be used when setting the operating conditions of the plant. The real power produced by a reactor can thus be hampered by inaccurate feedwater flow measurements and will be less than the power rating for the reactor. A 2% power derating costs a utility about $20,000 per day, or 7.3 $M per yr, in lost revenue for an 800 MWe unit at an energy cost of $0.05 per kW-hr. Overestimation of feedwater flow rates due to flow meter fouling has been reported to be the single most frequent cause of derating of pressurized water reactors (Nuclear News, 1993).

Venturi flow meters are the most commonly used device to measure the feedwater flow rate in nuclear power plant (Nuclear News, 1993). The flow meters consist of a short section of constricted flow area piping (the venturi surface) that is inserted between two flanges in the feedwater pipe. The purpose of the constriction is to accelerate the fluid and temporarily lower its static pressure. Pressure gauges are used for measuring the pressure drop between the inlet and constricted regions of the flow meter. The fluid flow rate is directly related to the measured pressure drop.

The accuracy of venturi flow meter measurements can decrease over time though, due to the deposition of corrosion products such as iron oxides and iron hydroxides in the feedwater flow onto the venturi surface. The degree of fouling and the nature of the deposits have been found to vary significantly from plant to plant and from flow meter to flow meter. The thickness of the deposits can differ from a few microns to a few hundred microns. Similar fouling problems have affected other types of differential-pressure feedwater flow rate measurement devices, such as flow nozzle, orifice plate, and elbow tap (Nuclear News, 1993).

The fouling of the venturi surface with corrosion products results in flow measurements becoming 1% - 2% higher than the actual flow. The onset of the fouling problem has been observed to develop early in the operating cycle, after as little as 2 months of operation with a clean flow meter. During long shutdown periods of the reactor, the feedwater flow meters are cleaned and recalibrated. But since the long shutdown periods occur at the end of a reactor operating cycle, which typically lasts for 18-24 months, reactors can spend most of their normal operating time with fouled feedwater flow meters (Mott and Blanch, 1992).

The Multivariate State Estimation Technique (MSET) computer code has been used to model one of the two venturi feedwater flow meters in Florida Power Corporation's Crystal River Unit 3 (CR-3) nuclear plant as a function of dissimilar process variables dynamically related to the feedwater flow rate. Argonne National Laboratory developed MSET to detect incipient disturbances of equipment, sensor, or operational parameters in nuclear plants with the objective of enabling the timely identification and scheduling of corrective actions. As part of the U. S. Department of Energy's ongoing effort to transfer innovations from its laboratories to U. S. companies, Argonne and Florida Power have been engaged in a collaborative study since 1992 to investigate the use of MSET for a variety of surveillance applications that include signal validation, instrument calibration monitoring, and early detection of component operability degradation (Gross, et. al., 1997).

MSET utilizes a nonlinear state estimation technique to model a physical process through the analysis of a group of sensors that monitor the process. The system model generated by MSET relies upon an examination of the totality of information available from the array of sensors used to monitor the system and a comparison of these data as a whole to similar sets of data collected from the same system operated at various conditions in the past. Based upon this comparison of the current condition of the system with its past history, an optimal estimate of the current state of the system is obtained even if there are errors in the data currently collected, i.e., some of the sensors have malfunctioned (Gross, et. al., 1997).

Description of the Model

The CR-3 plant contains two once-through steam generators to transfer heat from the primary system to the secondary system of the reactor. The flow rate of feedwater to the secondary-side of each steam generator is monitored by a venturi flow meter. Each of the two feedwater flow meters is located downstream of a feedwater pump that supplies condensate water to the loop A or loop B steam generator. Because the two loops contain identical components, only the feedwater flow meter in loop A has been modeled by MSET for the present investigation.

The loop A components from the inlet of the feedwater pump to the outlet of the steam generator are monitored by 29 sensors, including the flow meter. The loop A sensors, described in Table I, consist of steam generator level indicators, steam line thermocouples, feedwater thermocouples, steam line pressure transducers, feedwater pressure transducers, the feedwater pump tachometer, and the feedwater flow meter. Data from the first two months of the operating cycle that began in June of 1992 were used to determine the degree of correlation between each of the loop A diagnostic sensors and the feedwater flow meter. The correlation coefficient that reflects the degree of cross correlation between each of the sensor's signals and the feedwater flow rate is included in Table I. The sensors in Table I are sorted in decreasing order of their correlation coefficients. The sensors most highly correlated with the feedwater flow rate (i.e., those sensors with correlation coefficients greater than 0.9) are the steam generator level indicators, feedwater thermocouples, and steam line pressure transducers. These sensors tend to be those most highly correlated with the flow meter, regardless of which archive operating cycle data sets have been analyzed.

Description of the State Estimation Technique

The MSET state estimation technique is an advanced pattern-recognition technique that measures the similarity or overlap between signals within a defined operational domain. The MSET state estimation technique uses examples of the normal operating states of a system from which to learn relationships that exist between the parameters used to define the state. For each new observation of the system, it uses the patterns developed from the learned states to estimate the "true" state of the system. System states are represented by vectors whose elements are derived from sensor signals and can range from direct values of signals from the sensors to the result of any scalar transformation of the signals. Although the state vectors do not have to be linearly independent, they do have to represent the physical and/or chemical processes that are occurring and have some level of intercorrelation. The estimated state is calculated using a weighted combination of learned states, the weighting values being determined by the degree of pattern overlap with each learned state. (Singer, et. al., 1997).

If data are collected from some process over a range of operating states, these data can be arranged in matrix form, where each column vector in the matrix represents the measurements made at a particular state. Thus, this matrix will have the number of columns equal to the number of states (a total of **m** states) at which observations were made and the number of rows equal to the number of measurements (a total of **n** sensors) that were available at each observation. Defining the set of measurements taken at a given time $\mathbf{t_j}$ as an observation vector $\mathbf{X(t_j)}$,

$$X\left(t_j\right) = \left[x_1\left(t_j\right), x_2\left(t_j\right), \ldots, x_n\left(t_j\right)\right]^T, \tag{1}$$

where $x_i(t_j)$ is the measurement from sensor **i** at time t_j, then the data collection matrix can be defined as the process memory **D**:

$$\mathbf{D} = \begin{bmatrix} d_{1,1} & d_{1,2} & \cdots & d_{1,m} \\ d_{2,1} & d_{2,2} & \cdots & d_{2,m} \\ \vdots & \vdots & & \vdots \\ d_{n,1} & d_{n,2} & \cdots & d_{n,m} \end{bmatrix} \equiv \begin{bmatrix} x_1(t_1) & x_1(t_2) & \cdots & x_1(t_m) \\ x_2(t_1) & x_2(t_2) & \cdots & x_2(t_m) \\ \vdots & \vdots & & \vdots \\ x_n(t_1) & x_n(t_2) & \cdots & x_n(t_m) \end{bmatrix}. \tag{2}$$

Each of the column vectors in the process memory matrix represents an operating state of the system. Any number of observation vectors can be assigned to process memory matrix. Training of MSET consists of collecting enough observation vectors from historical operation of the system during normal conditions such that the process memory matrix encompasses the full dynamic operating range of the system.

Once the process memory matrix has been constructed, MSET is used to model the dynamic behavior of the system. At any point in time, an observation of the system ($\mathbf{X}_{obs}$) is made. MSET compares the current observation vector to the stored operating states to calculate an estimate of the current system state. The estimate of the current state ($\mathbf{X}_{est}$) is an **n**-element vector that is given by the product of the process memory matrix and a weight vector, **W**:

$$X_{est} = D \cdot W. \tag{3}$$

The weight vector represents a measure of similarity between the estimate of the current state and the process memory matrix. To obtain the weight vector, the error vector ϵ is minimized, where:

$$\epsilon = X_{obs} - X_{est}. \tag{4}$$

The error is minimized for a given state when:

$$W = \left(D^T \otimes D \right)^{-1} \cdot \left(D^T \otimes X_{obs} \right). \tag{5}$$

This equation represents a "least square" minimization when the operator $\otimes$ is the matrix dot product. The MSET method uses advanced pattern recognition techniques to determine the nonlinear operator $\otimes$ that fits the input data vector (Singer, et. al., 1997). Once the weight vector is found, the resulting estimate of the current state of the system is given by

$$X_{est} = D \cdot \left(D^T \otimes D \right)^{-1} \cdot \left(D^T \otimes X_{obs} \right). \tag{6}$$

For the venturi flow meter analysis, a variation of the MSET model described above is used. Because the flow meter is known to provide false measurements sometime following the first two months of an operating cycle, the flow meter signal is masked out of the calculation of the weight vector. Specifically, modified versions of the process memory matrix ($\hat{\mathbf{D}}$) and the observation vector ($\hat{\mathbf{X}}_{obs}$) are used to evaluate a modified weight vector ($\hat{\mathbf{W}}$):

$$\hat{W} = \left(\hat{D}^T \otimes \hat{D} \right)^{-1} \cdot \left(\hat{D}^T \otimes \hat{X}_{obs} \right). \tag{7}$$

The modified process memory matrix and observation vector are identical to those used in the standard form of the estimated state equation (i.e., Equation 3), except that the signals from the flow meter have been removed. The modified process memory matrix is given by

$$\hat{D} = \begin{bmatrix} d_{2,1} & d_{2,2} & \cdots & d_{2,m} \\ d_{3,1} & d_{3,2} & \cdots & d_{3,m} \\ \vdots & \vdots & & \vdots \\ d_{n,1} & d_{n,2} & \cdots & d_{n,m} \end{bmatrix} \equiv \begin{bmatrix} x_2(t_1) & x_2(t_2) & \cdots & x_2(t_m) \\ x_3(t_1) & x_3(t_2) & \cdots & x_3(t_m) \\ \vdots & \vdots & & \vdots \\ x_n(t_1) & x_n(t_2) & \cdots & x_n(t_m) \end{bmatrix}, \tag{8}$$

where the row of data corresponding to the flow meter (i.e., sensor number 1) has been removed. The modified weight vector is a function of signals from valid sensors only - the false signals reported by the flow meter have been masked out. The estimated state equation,

$$X_{est} = D \cdot \hat{W}. \tag{9}$$

still produces estimates of the flow meter signal because the modified weight vector acts on the original process memory matrix. As long as the process memory matrix contains valid flow meter data, collected from the flow meter before the flow meter begins to foul, the MSET estimates of the flow meter signal will reflect the true feedwater flow rate. When trained with reliable data, the MSET model can estimate the correct flow rate regardless of the changes in the physical state of the flow meter, since the model's estimates are based on the behavior of the system as a whole.

Results of the Analysis

For the MSET analysis of the CR-3 venturi flow meter, actual plant signals were taken from archive optical disks from the 18 month operating cycle spanning from June of 1992 through December of 1993. The CR-3 data acquisition system records signals from more than 1,000 plant sensors, including the 29 diagnostic sensors in loop A, at a rate of once per minute. For this analysis, only every tenth observation recorded during the reactor cycle was used (i.e., one observation every 10 minutes). But since the reactor run lasted 493 days, the total number of observation vectors available for training and testing of the model is over 67,000.

The MSET model utilizes data from all 29 diagnostic sensors in loop A. Figure 1 shows the signal from the feedwater flow meter for the whole of the operating cycle. The figure indicates which period of the operating cycle was used to train the model. Also indicated in Figure 1 is a roughly 2 month period near the middle of the cycle during which repairs were made to a multiplexor (MUX) unit in the data acquisition system. The signals recorded for all loop A sensors during this period were extremely erratic, and did not correspond to actual reactor conditions.

The MSET model was trained using data from the second month of the operating cycle (i.e., days 30 through 60). This period was selected for training of the model because it follows the startup phase of the operating cycle, during which sensor signals were erratic as various reactor components were tested and brought online, and it precedes the anticipated onset of flow meter degradation due to buildup of corrosion products. Training of the MSET model is a simple process which avoids time-consuming error minimization methods required to train neural networks. In MSET training, all that is necessary is the construction a process memory matrix (**D**) that represents the normal operating states of the modeled system. The MSET model is trained by selecting a subset of the data from the training period that spans all normal operating states of the system. MSET utilizes two algorithms to extract representative observation vectors from the training data. In the first algorithm, MSET selects training data that correspond to the extrema of the normal operating states. For each sensor, the algorithm finds the minimum and maximum sensor measurements from the training period data. The observation vectors containing these measurements are added to the process memory matrix. In the second algorithm, the remaining observation vectors from the training period are ordered by their Euclidean norms. The algorithm then selects evenly spaced elements from the ordered set and adds their corresponding observation vectors to the process memory matrix.

The MSET system, in contrast to neural networks, is able to produce extremely accurate estimates for the signals under surveillance with only a small subset of the available training vectors. For example, using only 100 training vectors, or 2.6% of the available training data, produces an root mean squared (rms) error of only 13 klbm/hr for the flow meter signal. Since the feedwater flow rate at full power is about 5,400 klbm/hr, the rms error of the calculated flow rate is only 0.24% of the feedwater flow rate at full power. As shown in Figure 2, the accuracy of the simulation, as measured by the root mean squared error of the calculated flow rate, becomes even greater as the number of observation vectors in the process memory matrix increases. Each of the points plotted in Figure 2 represents an individual MSET calculation for the training period. Because the accuracy of the simulation begins to level off for process memory matrices containing more than 400 observation vectors, a process memory matrix size of 500 observation vectors was selected as the standard model for the feedwater flow meter simulation. At a process memory matrix size of 500 observation vectors, the rms error of the calculated flow rate is 7.2 klbm/hr, which is only 0.13% of the feedwater flow rate at full power.

The flow meter error signal (i.e., the difference between the measured and calculated flow rates) is shown as a function of time in Figure 3 for the calculation whose process memory matrix contains 500 observation vectors. The error signal illustrates the great accuracy with which MSET has learned the training data. The flat response of the error signal during days 50 through 52 of the operating cycle is due to a gap in the recorded data.

In Figure 4, the calculated feedwater flow rate is shown for the time frame extending from the beginning of the training period (day 30) to the end of the operating cycle (day 493). The calculated flow rate (Figure 4) compares well with the measured flow rate (Figure 1), except during periods in which the feedwater flow rate falls below 2000 klbm/hr. On closer inspection though, a drift appears between the measured and calculated flow rates, as illustrated by Figure 5, which shows the difference between the measured and calculated flow rates. This drift is due to the fouling of the flow meter, which causes it to report flow rates that are greater than the calculated flow rates.

By the end of the eighth month of the operating cycle (day 240), the measured flow rate exceeds the calculated flow rate by roughly 60 klbm/hr, which is 1.1% of feedwater flow rate at full power. During the ninth and tenth months of the operating cycle (specifically, days 250 through 300), the difference between the measured and calculated flows is large, extending beyond the limits of the figure. During this period a multiplexor unit in the data acquisition system was replaced and some of the sensors used as inputs to the model were recalibrated. Because of the sensor recalibration, the training patterns in the process memory matrix are no longer valid, and this alters the character of the discrepancy between the measured and calculated flow meter signals. Evidence of resumption of the drift is nevertheless observed starting at about day 360. On-line retraining of the MSET model using post-recalibration data is feasible and straightforward.

Conclusions

The analysis of archived Crystal River-3 feedwater flow data reveals a slow and steady degradation of the flow meter measurements during the 1992/1993 operating cycle. MSET can reliably estimate the true flow rate and quantify the degree of departure between the indicated signal and the true flow rate with high accuracy. The MSET computed flow rate could, in principle, be used to provide an improved estimate of the reactor power and hence avoid the revenue loss associated with derating the reactor based on a faulty feedwater flow rate indication.

References

1. NUCLEAR NEWS, "Flow Rate Mismeasurement Causes Unneeded Derating, Vol. 36, No. 2 (February 1993) p. 39.

2. K. C. GROSS, R. M. SINGER, S. W. WEGERICH, J. P. HERZOG, R. VANALSTINE and F. BOCKHURST, "Application of a Model-Based Fault Detection System to Nuclear Plant Signals," *Proc. 9th Intl. Conf. on Intelligent Systems Applications to Power Systems*, Seoul, Korea (July 6-10, 1997).

3. K. KAVAKLIOGLU and B. R. UPADHYAYA, "Monitoring Feedwater Flow Rate and Component Thermal Performance of Pressurized Water Reactors by Means of Artificial Neural Networks," *Nuclear Technology*, Vol. 107 (July 1994) p. 112.

4. J. MOTT and P. BLANCH, "Feedwater Flow Estimation via Sample-Based Modeling," *Proceedings of the 8th Power plant Dynamics, Control and Testing Symposium*, Vol. 2, Knoxville, TN (May 27-29, 1992) p. 85.01.

5. R. M. SINGER, K. C. GROSS, J. P. HERZOG, R. W. KING and S. W. WEGERICH, "Model-Based Nuclear Power Plant Monitoring and Fault Detection: Theoretical Foundations," *Proc. 9th Intl. Conf. on Intelligent Systems Applications to Power Systems*, Seoul, Korea (July 6-10, 1997).

Table I. Loop A Diagnostic Sensors

Sensor Number	Sensor Tag	Description	Units	Corr. Coef.
1	S301	Steam Generator A Inlet Feedwater Flow Rate	klbm/hr	1.0000
2	S287	Steam Generator A Level (Startup Range)	inches	0.9974
3	S285	Steam Generator A Level (Full Range)	inches	0.9962
4	S284	Steam Generator A Level (Operating Range)	percent	0.9900
5	A322	Steam Generator A Level (High Range)	percent	0.9898
6	A321	Steam Generator A Level (Low Range)	inches	0.9863
7	S288	Steam Generator A Lower Downcomer Temp.	°F	0.9733
8	S254	Feedwater Pump A Discharge Temperature	°F	0.9563
9	S250	Feedwater Heater 6A Inlet Temperature	°F	0.9562
10	S256	Feedwater Pump A Suction Temperature	°F	0.9543
11	S265	Steam Generator Outlet 2A Pressure	psig	0.9450
12	S290	Steam Generator A Inlet Feedwater Temperature	°F	0.9352
13	S305	Steam Generator A Inlet Feedwater Temperature	°F	0.9352
14	S314	Steam Generator A Inlet Feedwater Temperature	°F	0.9351
15	S253	Feedwater Heater 6A Outlet Temperature	°F	0.9348
16	S307	Steam Generator Outlet 1A Pressure	psig	0.9341
17	W352	Steam Generator 3A Pressure	psig	0.9334
18	S309	Steam Generator A2 Upper Downcomer Temp.	°F	0.8966
19	A210	Feedwater Pump A Speed	rpm	0.8964
20	A315	Steam Generator A1 Upper Downcomer Temp.	°F	0.8897
21	S257	Feedwater Pump A Suction Pressure	psig	0.8827
22	A323	Steam Generator Outlet 1A Pressure	psig	0.8522
23	T228	Steam Generator Outlet 1A Pressure	psig	0.7674
24	S224	Steam Generator Outlet 1A Temperature	°F	0.7095
25	T227	Steam Generator Outlet 1A Temperature	°F	0.7029
26	S225	Steam Generator Outlet 2A Temperature	°F	0.6315
27	S255	Feedwater Pump A Discharge Pressure	psig	0.6096
28	T230	Steam Generator Outlet 2A Pressure	psig	0.3150
29	T229	Steam Generator Outlet 2A Temperature	°F	0.2852

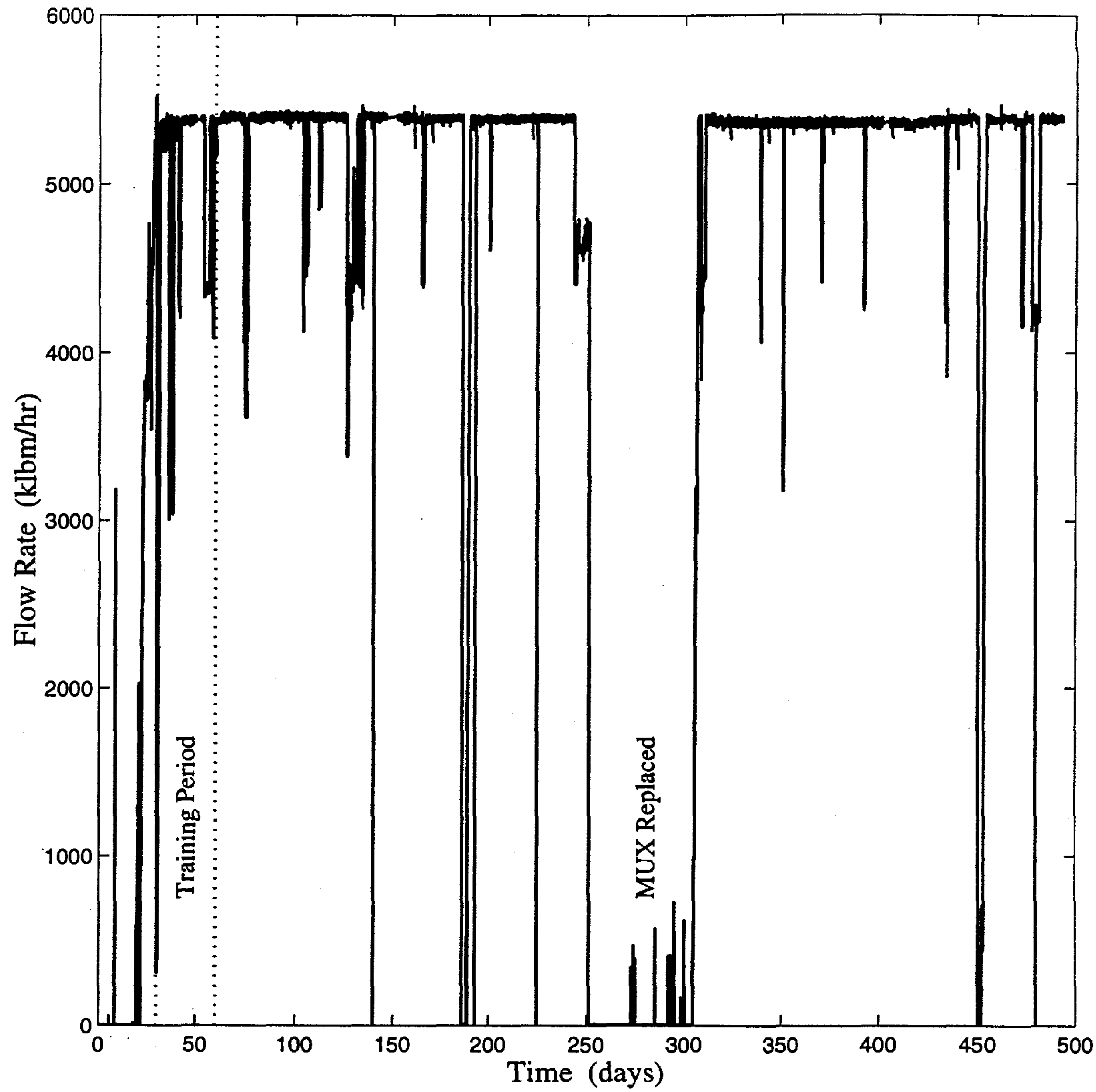

Figure 1. Flow Rate of the Loop A Flow Meter during the 1992/1993 Operating Cycle

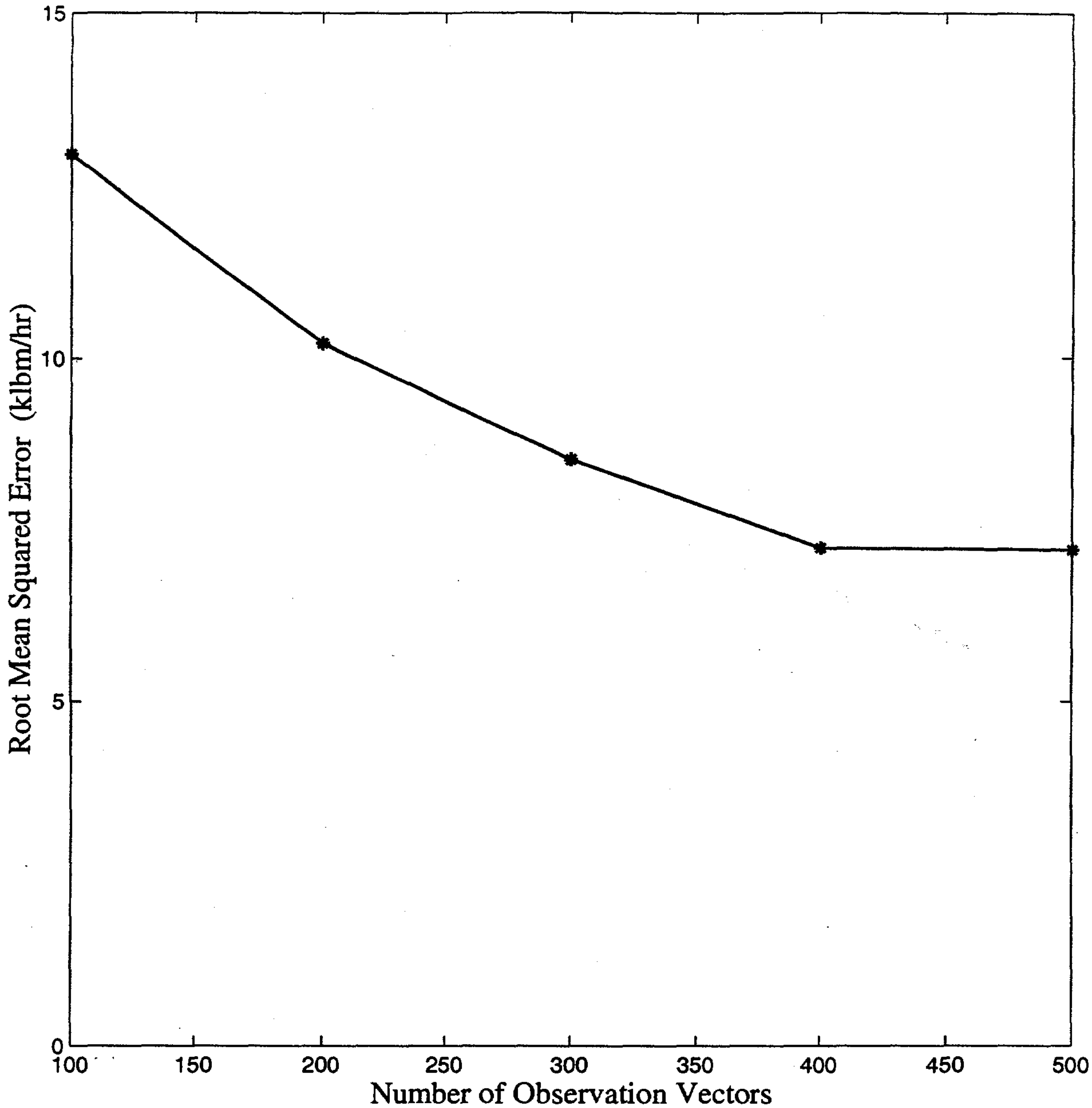

Figure 2. Root Mean Squared Error of the Calculated Flow Rate as a Function of the Number of Observation Vectors in the Process Memory Matrix

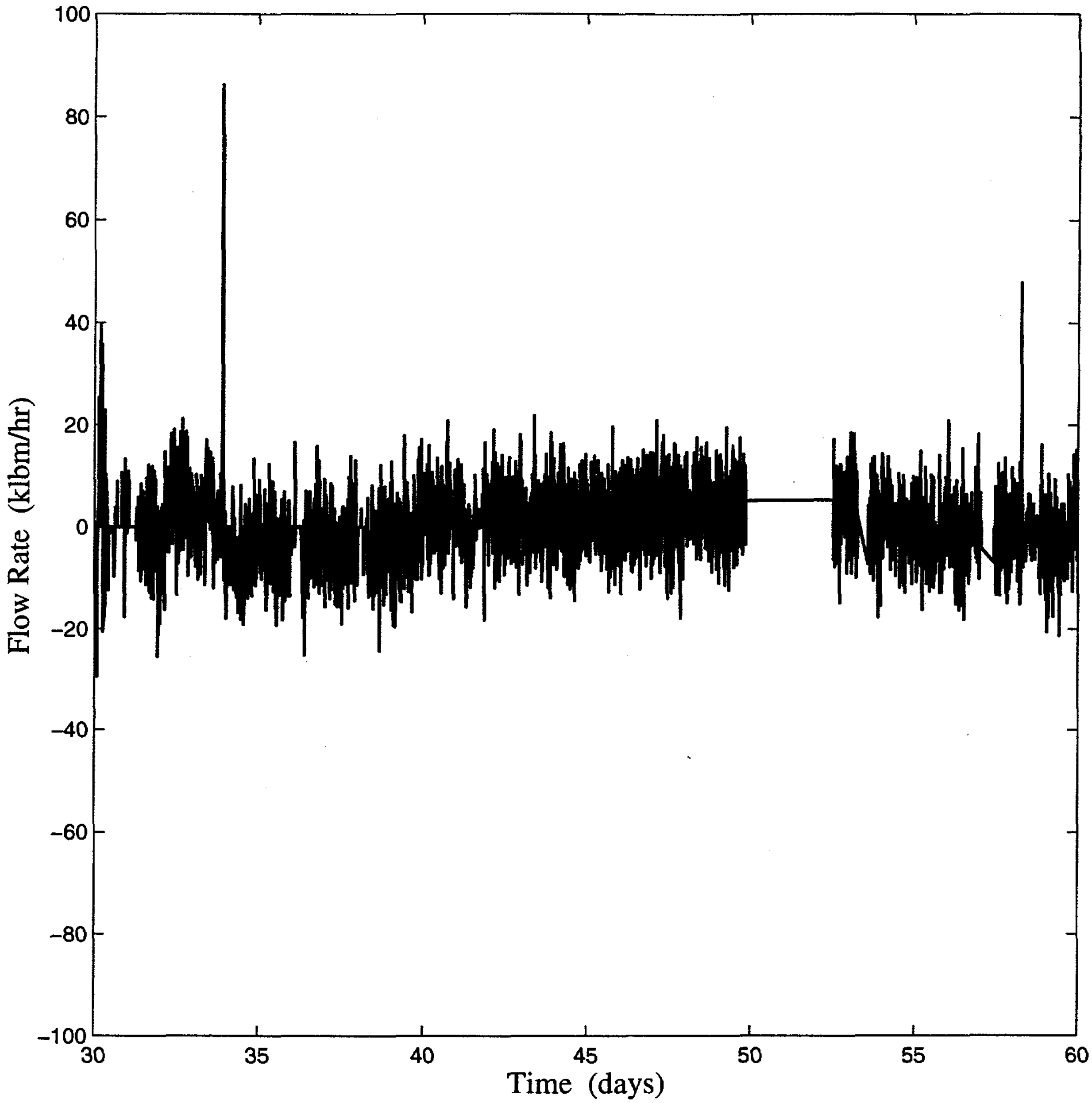

Figure 3. Difference between the Measured and Calculated Flow Rates for the Training Period.

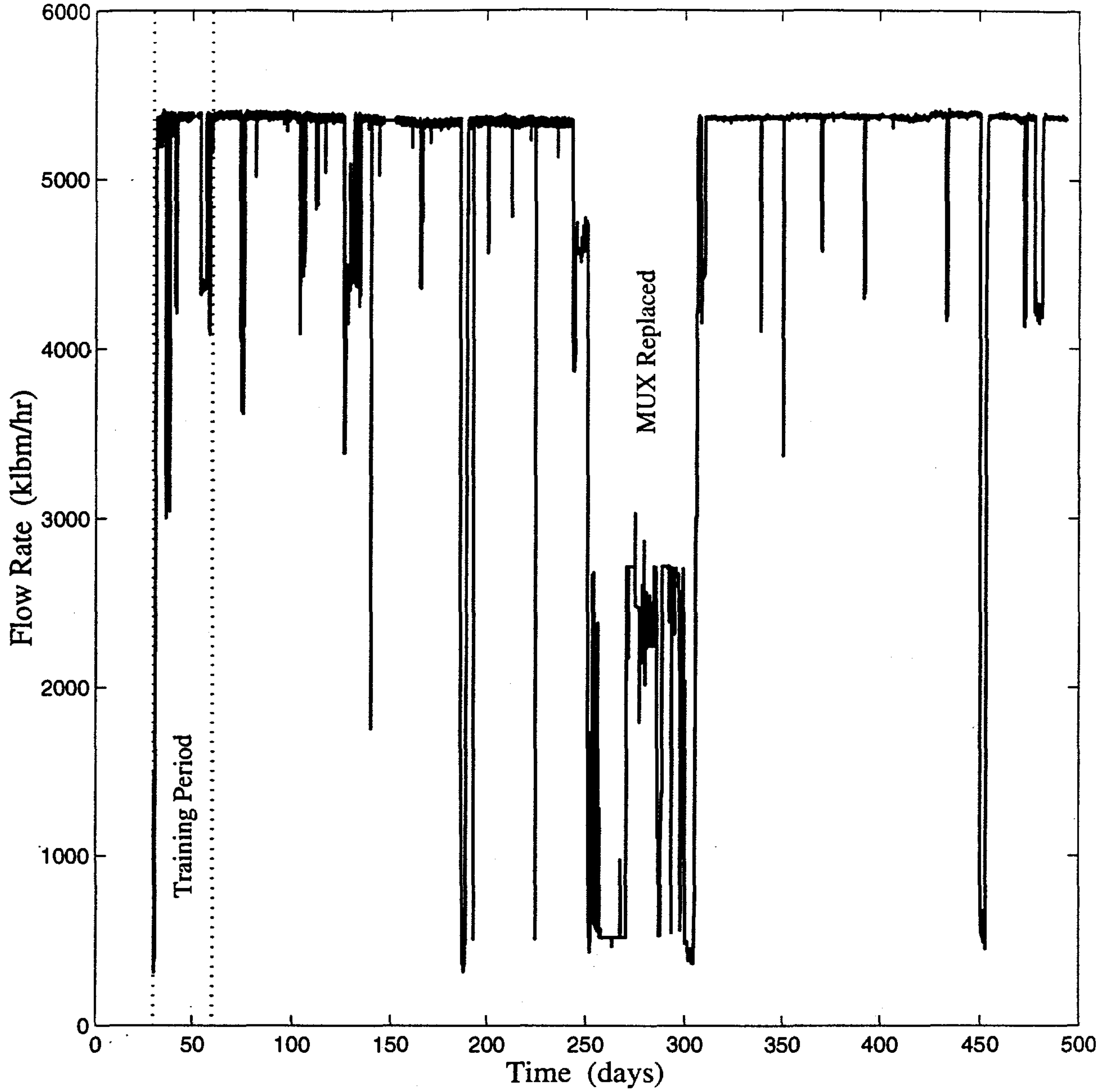

Figure 4. Calculated Flow Rate for the Loop A Venturi Flow Meter

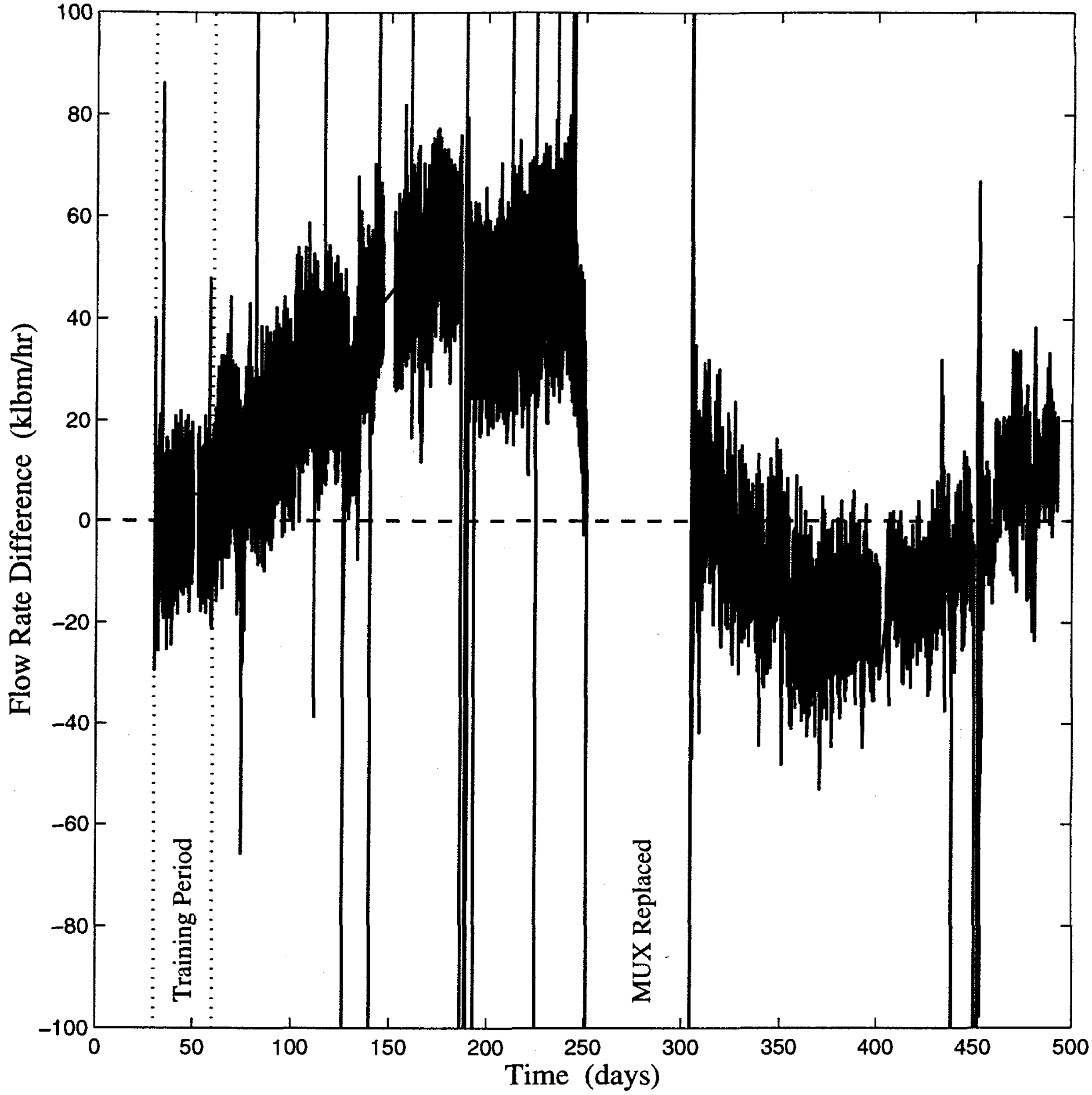

Figure 5. Difference between the Measured and Calculated Flow Rates